Intersystem Crossings of the Triplet and Singlet States in Cobalt and Copper Mononitrosyls

Ellie L. Uzunova*

Institute of General and Inorganic Chemistry, Bulgarian Academy of Sciences, Acad. G. Bonchev Str., bl. 11, Sofia 1113, Bulgaria

Received: July 23, 2009; Revised Manuscript Received: September 3, 2009

Local minima on the singlet, triplet, and quintet potential energy surfaces (PES) of cobalt and copper mononitrosyls are studied by DFT with the B3LYP functional. While quintet states are separated from the triplet and singlet states by a high energy gap, the linear singlet local minimum and the triplet transition state of CoNO lie close together. The ordering of local minima by relative stability of low-lying excited states with respect to the ground state was assessed by B3LYP, the coupled-cluster method CCSD(T), and complete active space calculations (CAS MP2). The ground state of CoNO is $^3A'$; two local minima were found in singlet states: linear, $^1\Sigma^+$, and side-on configuration, $^1A_1$. The occurrence of bound states on the triplet and singlet PES of CoNO and CuNO was examined by CASSCF. The crossing of the singlet and triplet PES of CoNO is a conical intersection; the geometry of the bound state is linear, with elongated N−O bond. The activation energy for the spin-forbidden transition $^3A' \rightarrow {}^1\Sigma^+$ is estimated to be 154.7 kJ mol^{-1}. For CuNO, the triplet and singlet PES do not cross but are separated by a small energy gap. Copper nitrosyl is of lower thermodynamic stability than cobalt nitrosyl. A triplet ground state $^3A''$ with bent configuration is predicted by B3LYP, confirmed by CAS MP2, and a very close-lying singlet state $^1A'$ is found with nearly identical geometry. Unlike CoNO, the linear triplet CuNO in $^3\Sigma^-$ state is not a transition state, but a local minimum, lying close to the dissociation limit Cu + NO. Vibrational frequencies are calculated for the gas-phase molecules and for the metal nitrosyl entrapped in solid Ar matrix. Under the influence of the noble gas matrix, the energy gap between the singlet and the triplet CuNO is reduced, and the singlet and triplet states of bent CuNO become nearly isoenergetic in agreement with experimental data. The linear CoNO in $^1\Sigma^+$ state is the most stable configuration in the Ar matrix, with one Ar atom coordinated to the metal center.

Introduction

The interaction of NO with transition metal atoms and cations of the 3d elements deserves interest from both experimental and theoretical viewpoint, because they are prospective as catalysts in the reduction of NO.[1−6] Copper-exchanged ZSM-5 is highly active in this reaction;[3] other cations and clusters of the 3d elements have been examined as well and considered as an alternative to the noble-metal catalysts for the deNO_x process.[4−6] The reaction parameters, however, are far from established, and the prediction of catalytic activity proves complicated: Cu(I) cations have much higher activity than Cu(II) cations; deactivation of the catalyst with time is responsible for inferior performance compared to metal catalysts and, particularly, noble metals.[3] In biological systems, similar processes occur in the degradation of toxins by metalloproteins.[2] A number of spectroscopic and theoretical studies have been devoted to the mononitrosyls of the 3d elements; nevertheless, the mechanism of the oxidative reduction in presence of transition metals or metal cations is not fully understood.[7−18] For the monocations of Sc and Ti, DFT studies predicted side-on geometries for the ground state mononitrosyls; linear ground states were found for the Cr−Co monocations, only the mononitrosyl of Cu^+ preferred a bent geometry.[17] The linear mononitrosyls MNO^+ (M = Fe, Co, Ni) were less stable than the side-on mononitrosyls formed by Sc and Ti at both the B3LYP and the CCSD(T) level of theory, but they were reported to have higher binding energies than the bent $CuNO^+$. Experimental data on the binding energies of the mononitrosyls are scarce, and the B3LYP calculated values are within the ranges determined by guided ion beam studies.[16,17] For the neutral mononitrosyls, a general trend was suggested, according to which the mononitrosyls from V to Cu would be bent in states of higher spin multiplicities, while they would be linear for the lowest multiplicity state.[7] More recent studies revealed that the ground state FeNO is indeed linear,[11,12] while nickel forms a bent mononitrosyl in a $^2A'$ ground state and also a stable side-on Ni-mononitrosyl.[9,12] In metal-nitrosyl coordination compounds of higher symmetry, for example, metal porphyrins or substituted carbonyls, the bent configuration of the M-NO center is a result of pseudo Janh-Teller instability of the linearly coordinated NO.[8,18,19] For the neutral cobalt and copper nitrosyls, the early theoretical studies could not unambiguously assign the ground state. CCSD calculations pointed to a triplet ground state of CuNO, while CCSD(T) favored a singlet ground state.[20] Later, DFT studies arrived at the same problem: pure density functionals were in favor of singlet states for both CuNO and CoNO, while hybrid functional studies assigned the triplet states as being of lower energy.[7,12,13] In all theoretical and spectral studies of CuNO, the energy gap between the triplet and the singlet state of CuNO was estimated as rather small, and the geometries at the two local minima were suggested to be quite similar.[10,13] Singlet to triplet transitions are forbidden, but they may become allowed by spin−orbit coupling. The crossing of two potential energy surfaces with the same multiplicity in polyatomic systems forms a (n-2) dimensional hyperline; for a triatomic system, this is an intersection line. However, the singlet to triplet crossing is of dimension (n-1).[21] The probability of spin-forbidden transitions depends on the magnitude of the spin−orbit coupling and the

* Corresponding author. E-mail: ellie@svr.igic.bas.bg.

10.1021/jp9069916 CCC: $40.75
Published on Web 09/29/2009

curvature of the potential energy surface at the points of crossing: conical intersection or avoided crossing.

The potential energy surfaces of cobalt and copper mononitrosyls have not been studied in detail. In the present study, the local and global minima of CoNO and CuNO in singlet, triplet, and quintet states have been determined by the B3LYP density functional method. A multiconfigurational study was performed by complete active space self-consistent method (CAS SCF) in order to determine the magnitude of spin−orbit coupling, to examine the occurrence and to evaluate the type of intersystem crossing. CCSD(T) and CAS MP2 calculations were also performed to validate the ordering of states with the B3LYP determined geometries. The thermodynamic stability, local magnetic properties, charge distribution, vibrational frequencies in the gas-phase and in an inert-gas Ar-matrix were also assessed.

Theoretical Approach

DFT calculations on metal nitrosyls MNO (M = Co, Cu) were performed with the hybrid B3LYP functional, which includes local and nonlocal terms as implemented in the Gaussian 03 package.[22−25] The 6-311G basis set expanded with diffuse functions, two sets of d-functions, and one set of f-functions was used for the TM atom centers; the 6-31G basis set, expanded with d and f polarization functions, was used for N, O, and Ar centers; the basis set for the adsorption complex reads as Cu, Co [10s21p20d14f9g], N [3s6p10d7f], O [3s6p5d7f], Ar [5s9p5d7f]. For validation of the choice of basis sets, B3LYP calculations with the 6-311+G(2df) basis for all atom centers have been performed on the singlet and triplet MNO; the optimized geometries changed insignificantly (largest deviation of 0.005 Å for bond lengths and 0.4° for bond angles; the ordering of states by stability did not change); this basis set would be however too expensive for the studies in Ar matrix and for CCSD(T) and CAS calculations. The harmonic vibrations of all optimized mononitrosyls were analyzed in order to reveal the nature of the stationary points obtained. The minima (local and global) on the potential energy surfaces (PES) were identified by the absence of negative eigenvalues in the diagonalized Hessian matrix; transition states were recognized by a single imaginary vibrational frequency. DFT calculations in spin-unrestricted mode often yield a solution, which does not correspond to the desired spin state but contains contributions from higher spin states. Spin contamination was estimated from the $\langle S^2 \rangle$ expectation values by treating the DFT orbitals as single-determinant Hartree−Fock wave functions. The triplet and singlet PES of CuNO and CoNO have been examined by a multiconfigurational study: CASSCF and CASMP2 with unrestricted natural orbitals. To validate the B3LYP ordering of states, coupled-cluster singles and doubles single-point calculations, including noniterative triples, CCSD(T),[26−28] and CAS MP2 calculations,[29−33] have been performed with the B3LYP-optimized geometries for the ground state and the low-lying excited states. The CAS optimizations, spin−orbit-coupling estimation and the studies of bound states[30,31] were done in a CAS(10,8) active space for CuNO (4a″−6a″)(15a′−19a′) and CoNO (4a″−6a″)(14a″−18a′); diffuse functions were not included in the basis set for these calculations. The symmetry of the molecule was not restricted during optimizations and full diagonalization of the CI matrix was performed; the spin−orbit and surface intersection calculations were state averaged for the singlet and triplet state with equal weights. The CAS MP2 calculations have been performed with 12 electrons and 10 active orbitals; Davidson diagonalization of the CI matrix was applied.[29−35]

TABLE 1: Calculated Bond Length (R), Dissociation Energy, Corrected for Zero-Point Energy (D_e), and Harmonic[a] Vibrational Frequency U for the NO Molecule

method	R_{N-O}, Å	D_e, kJ mol^{-1}	U, cm^{-1}
PW91[b]	1.166	702.0	1898
TPSS[b]	1.166	638.1	1898
TPSSh	1.158	609.8	1956
B3LYP	1.154	629.2	1982
expt, ref 42	1.1508	631.62 ± 0.18	1904

[a] Anharmonic correction: −26 cm^{-1} by the B3LYP method; −27 cm^{-1} by PW91. [b] Gaussian keywords used in the calculations: PW91PW91; TPSSTPSS.

Charges on atoms were calculated by natural population analysis and natural bond orbital analysis as implemented in Gaussian 03.[36,37] This method permits us to discern both covalent and noncovalent effects in molecules; the results are rather insensitive to basis set enlargement.

Vibrational frequencies of the ground-state clusters and the low-lying excited states were calculated at the B3LYP level of theory with the MNO molecule encaged by eight Ar atoms. The face-centered cubic cell of solid Ar cannot accommodate a metal nitrosyl without suffering strong distortion, and the presence of guest molecules in neighboring cells is very unlikely to occur. The primitive cell is too small to encage the nitrosyls, therefore cluster model calculations were performed with eight Ar atoms from the cubic supercell.[43] No coordinates have been fixed; the optimizations resulted in distortion of the Ar unit cell which accommodates the TM cluster. The frequencies of the imaginary vibrations, due to the incomplete cluster model and arising from movements of the Ar framework atoms only, did not exceed in absolute value 20 cm^{-1}.

Structure, Bonding, and Energetics of CoNO and CuNO

Binding of NO to Metals. The B3LYP density functional has been validated as appropriate method to study different types of nitrosyls.[11,13,17] In Table 1, B3LYP results on the molecular properties of NO are compared with results from pure density functionals without HF exchange (PW91), the more recent meta-GGA functionals (TPSS, and its hybrid variation, TPSSh).[38] Pure density functionals overestimate the NO bond length, but also the dissociation energy. TPSS predicts the same bond length as PW91, with improved dissociation energy; including 10% of exact exchange (TPSSh) shifts the dissociation energy too low. The B3LYP calculated NO bond length and dissociation energy agree with the experimental data; the calculated linear vibrational frequency, corrected for anharmonicity (−26 cm^{-1}) exceeds by 52 cm^{-1} the experimental value, while it is underestimated by PW91 and TPSS. Correction factors for the zero-point energies and vibrational frequencies are available for most basis sets[39] and the B3LYP determined frequency shifts upon coordination of NO to metal cations of the 3d elements, referred to the frequency of the gas-phase NO, proved to be correct.[10] B3LYP also gives the best prediction for the $CuNO^+$, $CuAr^+$, and $CuXe^+$ binding energies.[16]

The NO molecule is a ligand in numerous transition-metal complexes; it also substitutes CO in some penta- and tetracarbonyls.[1,6,13] NO is isoelectronic with O_2^+, it has one more electron than CO, which occupies the antibonding π^* orbital; the nitrogen atom however, is more electronegative than carbon. According to ESR spectral studies, 60% of the spin density belongs to the N atom.[40] The molecular electrostatic potential (MEP) map of NO indicates that the nitrogen atom has stronger electron-donor ability than oxygen, and the σ-orbital forms

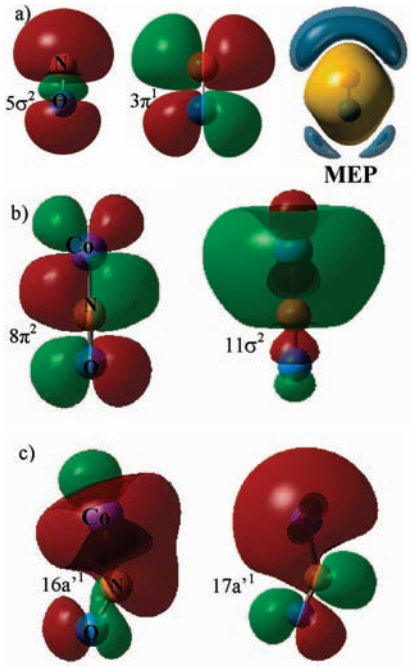

Figure 1. (a) The σ bonding orbital; the π* orbital; and the molecular electrostatic potential (MEP) map (au) of NO, derived from the DFT density; red and green colors represent the positive and negative parts of molecular orbitals; gradually decreasing yellow and blue colors represent positive and negative regions of the MEP map. (b) The $8\pi^2$ and $11\sigma^2$ MOs in linear CoNO,$^1\Sigma^+$ state. (c) The $16a'^1$ and $17a'^1$ MOs in bent CoNO, $^3A'$ ground state.

together with the partly occupied π* orbital a broad region of increased electron density around the N atom (see Figure 1a). The π component of the M-L bond with NO is much stronger than that with CO; consequently, while in carbonyls linear geometry is preferred, the nitrosyls are mostly bent. Binding of NO via the oxygen atom is less favorable; the MEP map indicates also that when NO is coordinated to the TM (transition metal) cation via the oxygen atom, the preferred structure will be bent, as the oxygen-to-metal charge transfer is much less efficient in a linear configuration. Linear nitrosyls can form only by binding of NO via the N atom, and the preference to linear or bent configuration in this case would be determined by the d-orbital occupancy of the TM. For symmetry reasons, in a linear configuration, the NO molecular σ orbital can interact only with the dz^2 atomic orbital of the transition metal, and the π* orbitals can interact only with the d_π orbitals: Figure 1b; in this case, the 4s AO contributes only to the σ bond. In the bent nitrosyls, the 4s and the dz^2 AO interact more efficiently with the d_π orbitals of NO: Figure 1c. NO binds to transition metals via a synergic mechanism in which a stronger bond is formed because of L → M charge transfer from the σ orbital of NO to unoccupied d orbitals of the transition metal and back-donation of electron density from the metal to the ligand via the overlap of occupied d_π orbitals of the metal with partly occupied antibonding p_π* orbitals of the ligand. As the extent of M → L back-donation increases, the M−L bond becomes stronger, while the N−O bond becomes weaker.

Cobalt Nitrosyl. Below the dissociation limit to Co + NO, four local minima and one transition state were found at the B3LYP level of study; see Figure 2. The N−O bond is weakened in all of the nitrosyl configurations, compared with the free NO molecule: Table 2. In singlet state, two local minima exist: (i) the $^1A'$ state has side-on geometry with a considerably lengthened N−O bond, and the Co atom binds to both the N and the O atom, with the Co−O bond being weaker; and (ii) a linear singlet $^1\Sigma^+$ in which both the Co−N bond and the N−O bond are with reduced length, compared with the other CoNO configurations. The ground state as determined by B3LYP is $^3A'$ and a linear transition state $^3\Sigma^+$ is located on the triplet PES; see Figure 3. Both of the triplet states are significantly spin-contaminated. CCSD(T) calculations favor the singlet states as more stable and denote the side-on singlet configuration as the ground state; however, the energy difference between the $^1A'$ side-on nitrosyl and the $^3A'$ bent nitrosyl is smaller than the value determined by B3LYP, not exceeding 0.5 eV. A side-on structure of CoNO has been detected experimentally by IR spectral studies in solid matrix (ω_{NO} 1284 cm^{-1} in Ar matrix),[12] but there is no evidence that this configuration could be of superior stability. CASSCF and CASMP2 calculations confirm the B3LYP ordering of states. The energy gaps between the side-on singlet state and the linear singlet state are smaller at

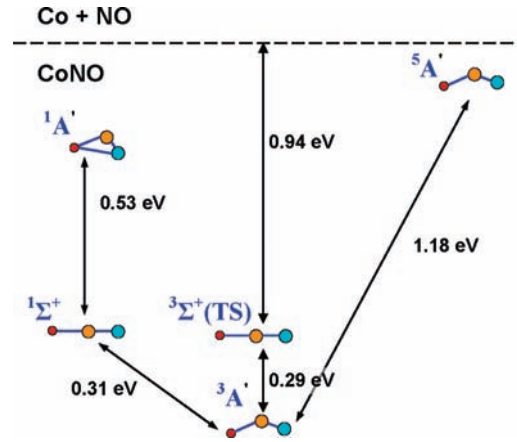

Figure 2. Ground state, low-lying local minima and transition states (TS) of CoNO, ordered as to their relative energies and grouped according to spin multiplicity. Co atoms are small red circles; N atoms, dark yellow circles; O atoms, large blue circles. The arrows (not to scale) denote the energy difference ΔE_{tot}, corresponding to adiabatic transitions (zero-point corrections included).

TABLE 2: Bond Lengths, Bond Angles, Energies[a], Zero-Point Energies (ZPE), Electron Spin Densities (ESD), Spin Contamination Expectation Value $\langle S^2\rangle$, Natural Orbital Occupancies; Natural Charges on Atoms and Linear Vibrational Frequency (ω_{NO}) for Cobalt Nitrosyl

state	$^1A'$	$^1\Sigma^+$	$^3A'$	$^3\Sigma^+$ (TS)	$^5A''$
R_{Co-N}, Å	1.658	1.553	1.710	1.689	1.831
R_{N-O}, Å	1.246	1.172	1.185	1.184	1.193
∠CoNO, deg	78.6	180.0	141.3	180.0	135.6
ESD_{Co}	0.00	0.00	2.35	1.52	2.70
ESD_N	0.00	0.00	−0.16	0.37	0.73
ESD_O	0.00	0.00	−0. 19	0.11	0.57
Co 3d	8.22	7.92	7.47	7.89	7.56
Co 4s	0.37	0.89	1.18	0.69	0.96
q_{Co}	0.38	0.20	0.35	0.37	0.40
q_N	−0.01	0.11	−0.11	−0.13	−0.18
q_O	−0.37	−0.31	−0.24	−0.24	−0.22
ω_{NO}	1404	1915	1722	1726	1667
$\langle S^2\rangle$○	0.000	0.000	2.540	2.438	6.025
$\Delta E_{tot} \times 10^2$ B3LYP	3.073	0.972	0.000	1.081	4.352
ZPE[b], kJ mol^{-1}	15.33	19.50	14.76	13.30	14.13
$\Delta E_{tot} \times 10^2$ CCSD(T)	−1.797	−1.080	0.000	1.260	n.c.
$\Delta E_{tot} \times 10^2$ CASSCF	1.806	1.021	0.000	1.613	n.c.
$\Delta E_{tot} \times 10^2$ CASMP2	10.985	2.275	0.000	4.120	n.c.

[a] ΔE_{tot}: total energy difference relative to the ground-state CoNO, E = −1512.639941 hartree (B3LYP). [b] B3LYP calculated zero-point energies. TS, Transition state. n.c., not converged.

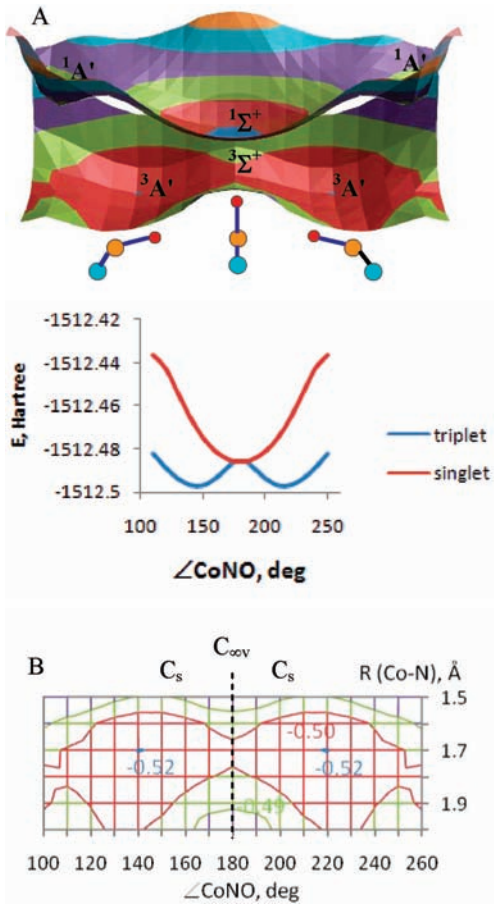

Figure 3. (A) 3D and 2D representation of triplet and singlet PES of CoNO, calculated by B3LYP with all local minima and the linear transition state $^3\Sigma^+$ denoted. (B) Contour diagram of CoNO in its ^{3}A′ state as a function of the internal coordinates R_{Co-N} and ∠CoNO with R_{NO} fixed at the value of the global minimum of PES. Energy values are scaled (E_{tot} +1512) × 10^2 Hartree.

the CASSCF level, indicating a smoother singlet PES; however, the CASMP2 calculated energies are in favor of the existence of deeper valleys containing the global minima for both the singlet and the triplet PES: Table 2.

According to the natural population analysis, in all electronic states, the $3d^{n+1}4s^1$ occupancy is favored over $3d^n4s^2$; this is most pronounced for the side-on structure ^{1}A′. The Co 4s AO in the side-on nitrosyl is less than 20% occupied, compared with higher occupancies for the other configurations. In the side-on nitrosyl, the Co atom forms two bonds, to nitrogen and to oxygen, but the Co−O bond is considerably longer, 1.867 Å, than the Co−N bond, 1.658 Å. The natural charge distribution indicates that a charge-transfer component dominates in the Co−O bond formation. The side-on coordination causes very significant electron redistribution at the Co atom: electron density is transferred from the σ orbital of NO to vacant 3d orbitals at Co via both nitrogen and oxygen. Back-donation from the metal to the ligand results in depopulation of the 4s orbital and increased local negative charge of the oxygen atom. The CoNO in the quintet ^{5}A″ state is bent; this is the least stable state, lying only 0.05 eV below the dissociation limit Co + NO. The bond N−O is slightly elongated, while the Co−N bond is longer by more than 0.1 Å compared with the triplet ground state. The electron spin density on the metal center and the charge distribution on atoms for the ^{5}A″ state and the ^{3}A′ state are similar: the Co atom bears a local magnetic moment arising from the dominant $3d^{n+1}4s^1$ occupancy. The triplet state is a result of antiferromagnetic coupling with the unpaired electron of NO.

TABLE 3: CAS Study of CoNO at the Point of Conical Intersection; Geometry Parameters, Energies and Spin-Orbit Coupling Constants

	CoNO
R_{Co-N}, Å	1.619
R_{N-O}, Å	1.338
E ($^1\Sigma^+$), Hartree	−1510.4678667
E ($^3\Sigma^+$), Hartree	−1510.4678849
$\Delta E(^3\Sigma^+)/(^1\Sigma^+)$, cm^{-1}	4
$H^{SO} = H_\perp$, cm^{-1}	264.5
ΔE, kJ mol^{-1} ^{3}A′ → $^1\Sigma^+$	154.7

According to the B3LYP results, the $^1\Sigma^+$ and $^3\Sigma^+$(TS) are separated by a very small energy gap: Table 2. The zero-point correction is higher for the linear singlet $^1\Sigma^+$, rendering it slightly above the triplet TS by energy. The shape of the triplet and singlet PES suggests the presence of either an avoided crossing or a conical intersection; see Figure 3. The linear transition state (TS) lies on a path connecting two identical bent configurations and a bending Co−N−O vibration brings the molecule into one of the two symmetrically located minima ^{3}A′ via the linear TS. The energy barrier for this spin-allowed transition, calculated at the B3LYP level is 28.3 kJ mol^{-1}; it is higher at the CAS level, 42.3 kJ mol^{-1}.

The spin−orbit coupling constants in the free NO molecule are not negligible (122−124 cm^{-1}); they have been determined experimentally by precise measurements of the bands $^2\pi_{1/2} \rightarrow {}^2\pi_{1/2}$; the subbands $^2\pi_{3/2} \rightarrow {}^2\pi_{3/2}$ and the satellite bands $^2\pi_{3/2} \rightarrow {}^2\pi_{1/2}$ (transition between vibrational levels 0 and 1) of the ground state $^2\Pi$.[41] CAS calculations prove that crossing of the singlet and triplet PES of CoNO occurs via a conical intersection (see Table 3) as the eigenvalues at the point of crossing differ by only 1.8 × 10^{-5} Hartree. Strong spin−orbit interaction is in favor of this spin-forbidden process. The geometry of CoNO at the surface crossing is linear: the bond Co−N is of length intermediate of that determined by B3LYP for the $^1\Sigma^+$ state (local minimum) and the $^3\Sigma^+$ (transition state); the bond N−O is strongly elongated. The stretching NO vibration can bring the cobalt nitrosyl from the singlet local minimum to the point of surface crossing, where the singlet and triplet states are separated by only 4 cm^{-1}. The activation barrier of the spin-forbidden transition reaction can be estimated as a difference between the energy at the minimum of the triplet potential energy surface, ^{3}A′, and the energy of the bound state (Table 2, 3); it has a high value as calculated by CAS, 154.7 kJ mol^{-1} and indicates a low probability for spin-flipping. The low-lying vibrational states would provide a path to the ground state bent triplet via the linear TS configuration; only high vibrational levels may lead to a spin-forbidden process. The shape of the crossing point area can be modified by additional coordination of atoms. In a solid inert gas matrix, the IR spectra indicate that the linear singlet is the dominant CoNO configuration.

Copper Nitrosyl. Copper nitrosyl is less stable than cobalt nitrosyl; the linear triplet $^3\Sigma^-$ state lies very close to the dissociation limit Cu + NO (−0.07 eV); see Figure 4. All Cu−N bonds are longer than the Co−N bonds, and except in the ^{1}A′ state, the N−O bonds are elongated as well. B3LYP calculations indicate that the singlet ^{1}A′ and the triplet ^{3}A″ state are separated by a small energy gap: Table 4. Unlike cobalt nitrosyls, the triplet states of CuNO are not spin contaminated. CCSD(T) calculations favor the singlet state as more stable, and the energy gap of about 0.3 eV is larger than the B3LYP determined value.

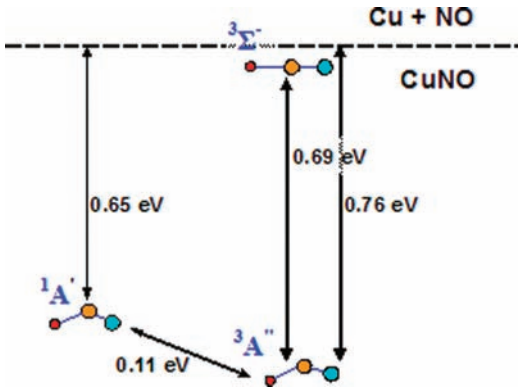

Figure 4. Ground state and low-lying local minima of CuNO, ordered as to their relative energies and grouped according to spin multiplicity. Cu atoms are small red circles; N atoms, dark yellow circles; O atoms, large blue circles. The arrows (not to scale) denote the energy difference ΔE_{tot}, corresponding to adiabatic transitions (zero-point corrections included).

TABLE 4: Bond Lengths, Bond Angles, Energies[a], Zero-Point Energies (ZPE), Electron Spin Densities (ESD), Spin Contamination Expectation Value $\langle S^2 \rangle$, Natural Orbital Occupancies; Natural Charges on Atoms, Linear Vibrational Frequency (ω_{NO}) and Spin-Orbit Coupling Constants H^{SO} for Copper Nitrosyl

state	$^1A'$	$^3A''$	$^3\Sigma^-$
R_{Cu-N}, Å	1.930	1.871	1.775
R_{N-O}, Å	1.177	1.196	1.214
∠CuNO, deg	118.8	129.7	180.0
ESD $_{Cu}$	0.00	0.55	0.25
ESD $_{N}$	0.00	0.81	0.99
ESD $_{O}$	0.00	0.64	0.76
Cu 3d	9.81	9.84	9.94
Cu 4s	0.96	0.68	0.12
q_{Cu}	0.22	0.43	0.90
q_N	−0.02	−0.21	−0.51
q_O	−0.20	−0.22	−0.39
ω_{NO}	1724	1651	1716
$\langle S^2 \rangle$	0.000	2.017	2.008
$\Delta E_{tot} \times 10^2$ B3LYP	0.375	0.000	2.300
ZPE[b], kJ mol^{-1}	14.80	13.72	19.62
$\Delta E_{tot} \times 10^2$ CCSD(T)	−1.210	0.000	1.901
$\Delta E_{tot} \times 10^2$ CASMP2	+1.010	0.000	3.451
H_x^{SO}; H_y^{SO}; $H_\perp^{SO}$	200.5; 49.2; 60.7		
H_{tot}^{SO}, cm^{-1}	215.2		

[a] ΔE_{tot}: total energy difference relative to the ground-state CuNO. E = −1770.390437 Hartree (B3LYP). [b] B3LYP calculated zero-point energies.

Both B3LYP and CASMP2 calculations denote the bent triplet state as the groundstate. The binding mechanism in CuNO is similar to that in CoNO. The $3d^{n+1}4s^1$ occupancy is dominant also in copper nitrosyls and results in a nearly closed d shell of the copper cation center. In the triplet state $^3A''$, we find a more distinct charge-transfer component from copper to the nitrogen atom than in the singlet state; this effect is further increased in the linear triplet state where the spin density of the molecule is allocated at the ligand mainly. In the $^3A''$ state, the spin density of the unpaired electron from the metal center is nearly equally shared by the metal and the ligand. Copper nitrosyl in a quintet state is endothermic (at +3 eV above the dissociation limit); configurations with NO bonded to the metal center via the oxygen atom also remain above the dissociation limit and have not been examined here.

A markedly different PES is revealed both for triplet and singlet state CuNO, compared with CoNO: Figure 5. At the

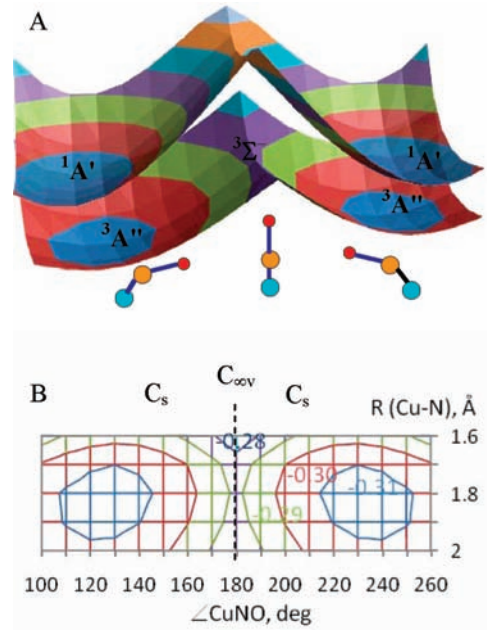

Figure 5. (A) 3D representation of triplet and singlet PES of CuNO, calculated by B3LYP with all local minima denoted. (B) Contour diagram of CuNO in its $^3A''$ state as a function of the internal coordinates R_{Cu-N} and ∠CuNO with R_{NO} fixed at the value of the global minimum of PES. Energy values are scaled $(E_{tot} + 1770) \times 10^2$ Hartree.

B3LYP level of theory the PES for triplet states lies below the one for singlet states; a stable linear configuration is found only in a triplet state $^3\Sigma^-$, but unlike CoNO, this is a local minimum, not a transition state. The CuNO in $^3\Sigma^-$ state has higher zero-point energy than that in all other states; see Table 4. Spin−orbit coupling for CuNO is comparable to that for CoNO in total magnitude; however, crossing of the triplet and singlet PES does not occur for CuNO. The linear triplet can be described as $Cu^+[NO]^-$, with a local charge at the copper atom 0.90. The N−O bond is lengthened; the Cu4s AO is considerably depopulated.

Vibrational Frequencies. The isolated mononitrosyls are of either C_s or $C_{\infty v}$ symmetry. The irreducible representations for bent and linear configurations respectively are $\Gamma(C_s) = 3a'(IR,R)$ and $\Gamma(C_{\infty v}) = 2\sigma^+(IR,R) + \pi(IR,R)$. The highest frequency vibration corresponds to a linear stretching of the N−O bond, and this vibration is manifested in the IR spectrum with highest intensity. The bending mode is of lowest energy; in linear configurations, it arises from the doubly degenerate π mode. All of the nitrosyls of the 3d elements were studied experimentally by trapping the species formed by the reaction of laser-ablated metal atoms with NO in inert noble gas matrix and recording the IR spectra of the matrix-isolated molecules.[10,12,13] IR studies of CuNO entrapped in solid Ne and Ar revealed two bent configurations of very close stability, and it was suggested that the origin of these states are the bent triplet $^3A''$ and singlet $^1A'$.[10] The cubic close-packed unit cell of solid Ar, with a lattice parameter of 5.256 Å and Ar−Ar interatomic distances of 3.717 Å[43] can host the metal nitrosyls upon distortion, thus forming a local defect. The presumed inert matrices in fact often interact with a transition metal center. In cases when direct coordination of atoms from the noble gas matrix is not observed, the matrix environment is able nevertheless to modify the ordering of states in metal oxide clusters of cobalt and nickel, for which near-degeneracy effects are significant.[44] Experimental studies provided evidence for coordination of up to two Ar or Xe atoms

TABLE 5: Harmonic Frequencies (ω) of Copper and Cobalt Nitrosyls in a Solid Ar Matrix, Type of the Adsorption Complex Formed with Inert Gas Atoms, and Metal−Ar Binding Energy BE(M-Ar), Calculated by B3LYP

cluster	ω (in Ar), cm^{-1}	ω(exp), cm^{-1}	adsorption complex	R_{M-N}; R_{N-O}, Å ∠MNO, deg	M−Ar distance, Å	BE(M-Ar), kJ mol^{-1}
CoNO; $^1\Sigma^+$	1914; 729; 369	1761; 620[a]	ArCoNO	1.559; 1.172	2.378	18.2
CoNO; $^3\Sigma^+$	1792; 554; 326; 201i		ArCoNO	1.674; 1.187	2.388	10.7
CoNO[c]; $^3A'$	1725; 487; 256			1.709; 1.187; 143.1°	3.302	
CuNO; $^3A''$	1631; 432; 224	1521; 512; 220[b]		1.865; 1.201; 130.0°	3.226	
CuNO; $^1A'$	1716; 473; 281	1587; 453; 278[b]		1.935; 1.179; 118.5°	4.040; 4.060	

[a] Reference 12. [b] References 10 and 13. [c] CoNO in a strongly distorted Ar unit cell; Ar−Ar = 6.8 Å.

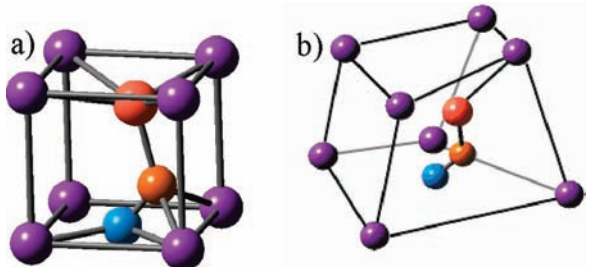

Figure 6. MNO cluster (CuNO; $^3A''$; inside the Ar cage), entrapped in the cubic unit cell of solid Ar. Argon atoms from the matrix are dark gray. Inner cluster: Cu, large light red sphere; N atom, dark yellow sphere; O atom, blue sphere. (a) Cluster model before optimization. (b) B3LYP optimized structure.

to dioxides of the 3d elements; the total binding energies were estimated to be in the range 50−60 kJ mol^{-1}.[45] In the present study, the metal nitrosyls were encaged in a cubic cell of eight Ar atoms from the cubic supercell and full relaxation was allowed; see Figure 6. A formal criterion for the assignment of a coordination complex with Ar is based on the formation of an M-Ar bond of length shorter than 3 Å. In the optimized structures, the shortest Ar−Ar distances are lengthened to 4.2 Å; stronger distortion was observed with CoNO in $^3A'$ state, for which the shortest Ar−Ar distance reached 6.8 Å.

Cobalt mononitrosyl is stable as a linear singlet in solid Ar; the linear triplet remains a transition state, and the $^3A'$ state is only stable in a much distorted Ar cell: Table 5. Both the $^1\Sigma^+$ and the $^3\Sigma^+$ states of CoNO coordinate a single Ar atom in a linear arrangement; the energy gap remains too small, 5.6 kJ mol^{-1}, and spin-flipping might be expected to occur. The bond lengths and the shape of the nitrosyls do not change significantly by the interaction with the matrix. The most significant alterations were found for CuNO in $^1A'$ state where the Cu−N bond is lengthened by 0.005 Å and for CoNO in $^1\Sigma^+$ state, with a Co−N bond lengthened by 0.006 Å. Though two of the Ar atoms from the matrix remain more closely positioned to CuNO clusters, the Cu−Ar distances are longer than 3 Å, and interactions are weak. The binding energies, calculated for Ar coordination to CoNO, agree with previously reported values for transition metal compounds, entrapped in Ar matrix.[45] The calculated stretching N−O vibrational frequency for CoNO in $^1\Sigma^+$ state is higher than the experimental value by 153 cm^{-1}; for the ground state $^3A'$, the calculated frequencies are slightly low. Assuming that spin flipping in the Ar-coordinated CoNO occurs, the lower experimental value can be attributed to a state constrained by the matrix and with slightly different geometry than the one determined for isolated CoNO. Similar differences between calculated and experimental values are found for CuNO; however, the frequency shifts of υ_{NO} for the two local minima $^3A''$ and the $^1A'$ (B3LYP, 85 cm^{-1}; expt, 66 cm^{-1}) are in good agreement with experiment. CCSD(T) single-point calculations of singlet and triplet CuNO in a cubic cell of eight Ar atoms, with geometries optimized at the B3LYP level indicated that the energy gap between the two local minima with different multiplicity is reduced to 18.1 kJ mol^{-1}.

Conclusion

Cobalt and copper mononitrosyls are studied by DFT with the B3LYP functional and by multiconfigurational approach in complete active space (CAS). Spin-forbidden transitions in cobalt nitrosyl are enabled via conical intersection of the triplet and singlet state potential energy surfaces. The CoNO molecule in its ground state $^3A'$ is bent, according to B3LYP and CASMP2 studies; other local minima are found in singlet states: linear and side-on nitrosyl. In a solid Ar gas matrix, used for gathering spectral information on transition metal nitrosyls, the linear singlet is the most stable form. Copper nitrosyl is of lower stability than cobalt nitrosyl; the triplet and singlet PES lie close to the dissociation limit. The geometries of bent CuNO in $^1A'$ and $^3A''$ states are not significantly different; the bond N−O is lengthened in the triplet state by 0.019 Å. Both CCSD(T) and B3LYP studies denote that the $^1A'$ and $^3A''$ states are separated by a small energy gap, which is further reduced upon interactions with atoms from Ar gas matrix.

Acknowledgment. The author gratefully acknowledges CPU time at the Computer Center, Technical University, Vienna, where most of the Gaussian 03 calculations were performed.

References and Notes

(1) Richter-Addo, G. B.; Legzdins, P. *Metal Nitrosyls*; Oxford University Press: New York, Oxford, 1992.
(2) Wink, D. A.; Grisham, M. B.; Mitchell, J. B.; Ford, P. C. *Methods Enzymol.*; Packer, L., Ed.; Academic Press: San Diego, 1996; Vol 268.
(3) Kuroda, Y.; Iwamoto, M. *Top. Catal.* **2004**, *28*, 111.
(4) Li, Y.; Hall, W. K. *J. Phys. Chem.* **1990**, *94*, 6145.
(5) Beutel, T.; Sárkány, J.; Lei, G.-D.; Yan, J.; Sachtler, W. M. H. *J. Phys. Chem.* **1996**, *100*, 845.
(6) Heyden, A.; Hansen, N.; Bell, A. T.; Keil, F. J. *J. Phys. Chem. B* **2006**, *110*, 17096.
(7) Blanchet, C.; Duarte, H. A.; Salahub, D. R. *J. Chem. Phys.* **1997**, *106*, 8778.
(8) Fenske, R. F.; Jensen, J. R. *J. Chem. Phys.* **1979**, *71*, 3374.
(9) Bauschlicher, C. W., Jr.; Bagus, P. S. *J. Chem. Phys.* **1984**, *80*, 944.
(10) Krim, L.; Manceron, L.; Alikhani, M. E. *J. Phys. Chem. A* **1999**, *103*, 2592.
(11) Gutsev, G. L.; Mochena, M. D.; Johnson, E.; Bauschlicher, C. W., Jr. *J. Chem. Phys.* **2006**, *125*, 194312.
(12) Zhou, M.; Andrews, L. *J. Phys. Chem. A* **2000**, *104*, 3915.
(13) Zhou, M.; Andrews, L. *J. Phys. Chem. A* **2000**, *104*, 2618.
(14) Cassady, J. C.; Freiser, B. S. *J. Am. Chem. Soc.* **1985**, *107*, 1566.
(15) Khan, F. A.; Steele, D. L.; Armentrout, P. B. *J. Phys. Chem.* **1995**, *99*, 7819.
(16) Koszinowski, K.; Schröder, D.; Schwarz, H.; Holthausen, M. C.; Sauer, J.; Koizumi, H.; Armentrout, P. B. *Inorg. Chem.* **2002**, *41*, 5882.
(17) Thomas, J.; Bauschlicher, C. W., Jr.; Hall, M. B. *J. Phys. Chem. A,* **1997**, *101*, 8530.
(18) Bersuker, I. B. *Electronic Structure and Properties of Transition Metal Compounds: Introduction to the Theory*; John Wiley & Sons: New York, 1996.
(19) Albright, T.; Burdett, J.; Whangbo, M.-H. *Orbital Interactions in Chemistry*; J. Wiley & Sons: New York, 1985.
(20) Hrušák, J.; Koch, W.; Schwarz, H. *J. Chem. Phys.* **1994**, *101*, 3898.

(21) (a) Yarkony, D. R. *Rev. Mod. Phys.* **1996**, *68*, 985. (b) Yarkony, D. R. *J. Am. Chem. Soc.* **1992**, *114*, 5406. (c) Ragazos, I. N.; Robb, M. A.; Olivucci, M.; Bernardi, F. *Chem. Phys. Lett.* **1992**, *197*, 119.
(22) Frisch, M. J.; Trucks, G. W.; Schlegel, H. B. Gaussian 03, Revision D.01; Gaussian, Inc.: Wallingford, CT, 2004.
(23) Lee, C.; Yang, W.; Parr, R. G. *Phys. Rev. B* **1988**, *37*, 785.
(24) Miehlich, B.; Savin, A.; Stoll, H.; Preuss, H. *Chem. Phys. Lett.* **1989**, *157*, 200.
(25) (a) Becke, A. D. *J. Chem. Phys.* **1993**, *98*, 5648. (b) Becke, A. D. *J. Chem. Phys.* **1996**, *104*, 1040.
(26) Pople, J. A.; Krishnan, R.; Schlegel, H. B.; Binkley, J. S. *Int. J. Quantum Chem.* **1978**, *XIV*, 545.
(27) Cizek, J. *Adv. Chem. Phys.* **1969**, *14*, 35.
(28) Purvis, G. D.; Bartlett, R. J. *J. Chem. Phys.* **1982**, *76*, 1910.
(29) McDouall, J. J.; Peasley, K.; Robb, M. A. *Chem. Phys. Lett.* **1988**, *148*, 183.
(30) Hegarty, D.; Robb, M. A. *Mol. Phys.* **1979**, *38*, 1795.
(31) Eade, R. H. E.; Robb, M. A. *Chem. Phys. Lett.* **1981**, *83*, 362.
(32) Frisch, M. J.; Ragazos, I. N.; Robb, M. A.; Schlegel, H. B. *Chem. Phys. Lett.* **1992**, *189*, 524.
(33) Abegg, P. W. *Mol. Phys.* **1975**, *30*, 579.
(34) Bearpark, M. J.; Robb, M. A.; Schlegel, H. B. *Chem. Phys. Lett.* **1994**, *223*, 269.
(35) Bernardi, F.; Robb, M. A.; Olivucci, M. *Chem. Soc. Rev.* **1996**, *25*, 321.
(36) Reed, A. E.; Curtiss, L. A.; Weinhold, F. *Chem. Rev.* **1988**, *88*, 899.
(37) Weinhold, F.; Carpenter, J. E. *The Structure of Small Molecules and Ions*; Plenum, 1988; p *227*.
(38) (a) Toulouse, J.; Adamo, C. *Chem. Phys. Lett.* **2002**, *362*, 72. (b) Mattsson, A. E. *Science* **2002**, *298*, 759.
(39) (a) Scott, A. P.; Radom, L. *J. Phys. Chem.* **1996**, *100*, 16502. (b) http://cccbdb.nist.gov/vibscalejust.asp.
(40) Enemark, J. H.; Feltham, R. D. *Coord. Chem. Rev.* **1974**, *13*, 339.
(41) (a) James, T. C.; Thibault, R. J. *J. Chem. Phys.* **1964**, *41*, 2806. (b) James, T. C. *J. Chem. Phys.* **1964**, *40*, 762.
(42) Handbook of Chemistry and Physics, 85^{-th} ed.; CRC Press: Boca Raton, FL, 2004−2005.
(43) Henshaw, D. G. *Phys. Rev.* **1958**, *111*, 1470.
(44) Uzunova, E. L.; Mikosch, H.; Nikolov, G. *J. Chem. Phys.* **2008**, *128*, 094307.
(45) Zhao, Y.; Gong, Y.; Chen, M.; Zhou, M. *J. Phys. Chem. A* **2006**, *110*, 1845.

JP9069916